First stages of silicon oxidation with the activation relaxation technique

Patrick Ganster,[1] Laurent Karim Béland,[2] and Normand Mousseau[2]

[1]*Laboratoire Claude Goux, Centre SMS, CNRS UMR5146, Ecole Nationale Supérieure des Mines, 158 Cours Fauriel, 42023 Saint-Etienne, France*

[2]*Département de physique and Regroupement québécois sur les matériaux de pointe, Université de Montréal, C.P. 6128, Succursale Centre-Ville, Montréal, Québec, Canada H3C 3J7.*

Using the ART NOUVEAU method, we study the initial stages of silicon oxide formation. After validating the method's parameters with the characterization of point defects diffusion mechanisms in pure Stillinger-Weber silicon, which allows us to recover some known results and to detail vacancy and self-interstitial diffusion paths, the method is applied onto a system composed of an oxygen layer deposited on a silicon substrate. We observe the oxygen atoms as they move rapidly into the substrate. From these ART NOUVEAU simulations, we extract the energy barriers of elementary mechanisms involving oxygen atoms and leading to the formation of an amorphouslike silicon oxide. We show that the kinetics of formation can be understood in terms of the energy barriers between various coordination environments.

I. INTRODUCTION

With considerable technological efforts in place to decrease the size and thickness of nanoelectronic devices, we require a better understanding of the early stage formation of multilayered stacks in order to predict the structure and the matter organization associated with even smaller systems. This is the case, for example, of the SiO_2 layers formed by the oxidation of an Si substrate. This compound is one of the most widely used as a gate material in devices. Yet, despite a large number of experimental studies on the formation of this SiO_2 oxide, there is still very little understanding regarding the details of its early stage of growth[1–3] In this context, it is essential to develop new predictive numerical atomic-scale tools for the relevant scale of future devices. Here, we focus on the study of the formation of silicon oxide on a silicon substrate using the ART NOUVEAU method,[4–6] a fast and efficient algorithm for the unbiased exploration of the energy landscape as oxygen atoms are deposited on the substrate.

The initial stages of silicon oxidation are characterized by a structural reorganization of the substrate as a transition from 2×1 to 1×1 Si surface structure as shown by low energy electron diffraction.[1] The oxygen coverage of the surface is temperature dependent as Langmuir-type adsorption is observed at 820 K, as well as two-dimensional island growth at 920 K.[2] Extensive layer-by-layer growth of SiO_2 oxide by successive oxidation of Si planes, followed by atomic force microscopy,[3] reveals that the oxidation starts with SiO_2 islands joining together in a two-dimensional spreading. The growth continues at the interface as oxygen atoms start diffusing through the oxide inducing a layer-by-layer inner formation of silicon oxide. In all cases, it can be noted that the formed oxide is in an amorphous state with a very abrupt SiO_2/Si interface defined by a roughness extending at most over a few Si planes.[7]

In the past, a number of groups have simulated atomistic SiO_2 on Si growth using empirical laws deduced from experiments for the oxygen insertion in the substrate.[8–10] No direct simulation of the insertion has been performed yet, however, and the ART NOUVEAU method, used here, is a powerful tool to overcome this limitation by modeling directly the oxide formation, as the system explores its energy landscape. Providing unbiased access to diffusion mechanisms and energy barriers associated with oxygen migration, ART NOUVEAU is an ideal method for determining structural and configurational quantities, such as formation and migration energies of point defects and impurities, quantities that are generally difficult to obtain in low-symmetry problems.[6,11–14]

In this paper, we are interested in identifying the migration mechanisms and barriers for the oxygen insertion in crystalline silicon. We first describe the details of the simulation procedure and demonstrate the applicability of ART NOUVEAU to Stillinger-Weber crystalline silicon by looking at point defect—vacancy and interstitial—diffusion. We then apply the method to study oxygen migration into the bulk after these atoms are deposited at the surface of a silicon substrate. The resulting events allow us to identify energy ranges associated with various configurations as well as the most favorable local environments during the initial stages of the oxygen insertion.

II. SIMULATION DETAILS

ART NOUVEAU is an open-ended algorithm that generates pathways connecting adjacent local energy minima through an unbiased open search for first-order saddle points.[4–6] The generation of one event, defined as the identification, from a known initial local minimum, of an adjacent transition state and its connected final local minimum, takes place in three steps. (1) Starting for the initial energy minimum, a local atom and its neighborhood is selected. This set is displaced along a random vector until a direction of negative curvature on the energy surface appears. (2) The system is then moved along the eigenvector associated with the negative eigenvalue while the energy is minimized in the perpendicular $3N - 1$ dimensional hyperplane. The iteration stops when the total force approaches zero, indicating that a first-order saddle point has been reached. (3) The system is pushed over the transition state and is relaxed into an adjacent local energy minimum. These three steps generate an event. For structural evolution, events are accepted or rejected using a Metropolis scheme

based on the energy difference between the initial and final minima:

$$p_{\text{accept}} = \min[e^{-(E_{\text{fin}}-E_{\text{ini}})/k_B T}, 1], \qquad (1)$$

where T is a Metropolis temperature. Because vibrational entropic contributions are not included, this temperature should be considered as "fictitious," in the sense that it does not correspond to specific physical temperature. It is nevertheless possible to thermalize the system at this temperature.

ART NOUVEAU's parameters are described extensively in Ref. 14. Its implementation, which includes a number of improvements with respect to the initial algorithm, is discussed in Refs. 6 and 15. Comparisons with other saddle-point search algorithms show that ART NOUVEAU is an efficient method for open-ended searches, with 300 to 600 force evaluations per successful event.[6]

ART NOUVEAU is applied here to two systems: self-defect diffusion in crystalline silicon (cSi) and the formation of SiO_2 oxide at the surface of a slab of cSi.

Both systems are described using the Stillinger-Weber empirical potential form.[16] The original parameter set is used for the pure silicon phase while the Si-O interactions are taken from the work of Watanabe *et al.*.[8] This Watanabe potential has been used for successfully describing SiO_2 amorphous oxide on Si substrates and the structure of the SiO_2/Si interface,[17,18] and oxygen diffusion in SiO_2 oxide[19] as well as the resulting strain in the substrate during silicon oxidization.[9] We propose here to use this potential to study SiO_2 oxide formation starting from an oxygen layer deposited on a Si substrate.

Many other potentials have been proposed for SiO_2/Si systems,[20–23] as well as a very recent one developed by Philipp and collaborators.[24] As far as we know, no potential provides an exact description of this interface and of its kinetics of formation. We have selected the Stillinger-Weber (SW) form for continuity with our previous works but also because it avoid artifacts, such as those observed in Tersoff-like potential, due to a short cutoff radius, artifacts that may introduce energy discontinuity during atomic diffusion.[25]

III. PRELIMINARY TESTS: SELF-DIFFUSION OF SI

In order to demonstrate ART NOUVEAU's performance on Stillinger-Weber cSi, we first look at self-defect diffusion, a process that has been previously characterized by various other approaches.[26,27] The ART NOUVEAU scheme is applied to a 512-atom 21.72 Å cubic box with periodic boundary conditions containing either a vacancy (-1 atom) or an interstitial ($+1$ atom) initially positioned in a tetrahedral site.[27] For both systems, starting from a defect configuration relaxed into a local energy minimum, we apply the ART NOUVEAU scheme with a Metropolis temperature of 0.4 eV in the case of vacancy diffusion and 2 eV in the interstitial diffusion. For vacancy diffusion, the set of atoms involved in an event is randomly chosen out of the four threefold coordinated Si atoms surrounding the vacancy and their nearest neighbors located within a cutoff radius of 6 Å. For interstitial diffusion, the set of atoms involved in an event corresponds to the interstitial atom and its near neighbors located within the same cutoff radius. Statistics on acceptation rate and parameters used in the simulations are resumed in Table I.

TABLE I. Statistics of ART attempts for the vacancy and interstitial systems. The number of ART events refers to successful ART attempts leading to a first-order saddle point. Events are classified as leading to the same state ($E_f = E_i$) or to states with different energies.

	Vacancy	Interstitial
Number of ART events	300	1200
Boltzmann weight (eV)	0.4	0.4
Number of accepted events	300	965
Cutoff radii (Å)	6	6
Number of events such $E_f < E_i$	0	309
Number of events such $E_f = E_i$	300	345
Number of events such $E_f > E_i$	0	311

Among the 300 ART attempts realized for the vacancy case and the 1200 attempts for the interstitial one, we observe a 100 and 80% success rate for the generation of events for vacancy and interstitial, respectively. This means that between 80 and 100% of initiated events converge to a first-order saddle point. Failed events are typically associated with the presence of a shoulder in a more complex energy landscape.[6]

Figure 1 presents the distribution of energy differences between the initial and the final minima (ΔE) for accepted events (top panels) and the corresponding distribution of associated energy barriers (bottom panels) for vacancy and interstitial diffusion. Vacancy diffusion is rather featureless, as expected. After crossing a 0.15 eV energy barrier leading to the ground state ($E_f - E_i = -1.66$ eV), all successful events correspond to the vacancy migration with an unique single energy barrier of 0.5 eV (single peak on the left panels of Fig. 1).

The interstitial energy landscape is more complex due to the presence of a number of metastable states. Starting with a Si atom placed in a tetrahedral interstitial site, associated with a formation energy of 5 eV, the first event corresponds
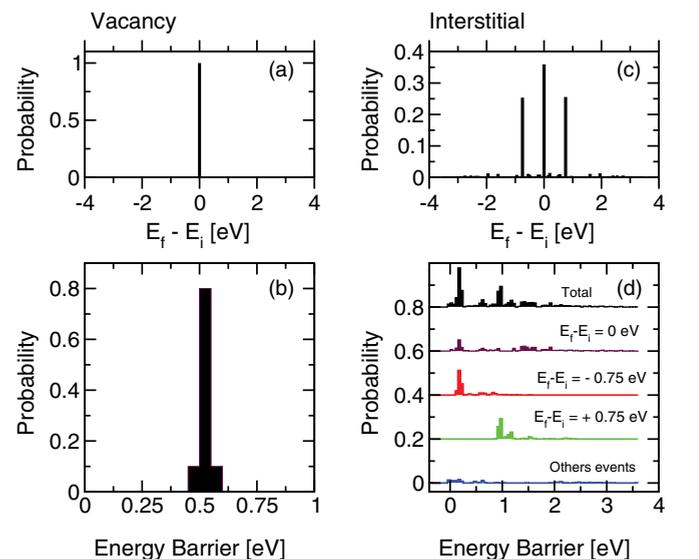

FIG. 1. (Color online) Top: Energy differences between the final and initial states for the (left) vacancy and (right) interstitial in crystalline silicon for accepted events. Bottom: Energy barriers (saddle minus initial state) for the same system.
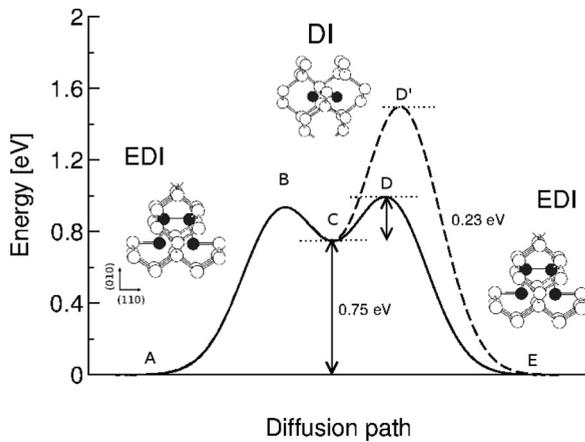
FIG. 2. Schematic of the energy barriers along the interstitial diffusion path. From EDI to EDI site (the most stable state), the DI site is a transitional configuration along the most probable energy barriers represented in the full line (ABCDE pathway). The CD'E pathway (dashed line) corresponds to less favorable events occurring from the DI to EDI site.

to a jump to a dumbbell insterstitial (DI) configuration with a formation energy of 4.44 eV. From this dumbbell position, the systems moves to the extended dumbbell interstitial (EDI) configuration, the most stable state for a Stillinger-Weber single interstitial with a formation energy of 3.68 eV. Diffusion then continues with the interstitial moving between two sites—the EDI and the excited DI configuration at 4.44 eV—with three barriers: 0.92 eV for the EDI to excited DI and 0.2 eV for the reverse. Figure 1(c) shows the distribution of energy differences between the initial and the final minima which present three peaks at −0.75 V, 0 eV and 0.75 eV corresponding to the jumps between the sites DI and EDI during diffusion. The three main peaks at 0.2, 0.7, and 0.95 eV are clearly identified on the partial distributions of Fig. 1(d). Analysis of the successive atomic configurations during the ART NOUVEAU exploration confirms that the DI site is a transitional configuration that occurs on the pathways from EDI to EDI site. The most probable energy barriers from EDI to EDI site with the transitional DI site are summarized in Fig. 2. The (CBA, CDE) and (ABC, EDC) paths correspond to $\Delta E = -0.75$ eV and $\Delta E = +0.75$ eV appearing in Fig. 1(c) with the corresponding energy barriers deduced from the Fig. 1(d). The dashed line (CD'E pathway) in Fig. 2 is associated with events found in the total distribution and the distribution with a $\Delta E = -0.75$ eV.

The partial distribution of energy barriers that peaks at $\Delta E = 0$ eV corresponds to events connecting directly two EDI or DI sites involving high energy barrier values. The smaller energy barrier values are associated with events where the systems comes back to the initial state from the saddle point (14% of the events).

These results are consistent with the energy barrier for interstitial diffusion of ∼ 0.8 eV obtained by molecular dynamics simulations at different temperatures,[26,27] since the higher 1.6 eV barrier, found without any bias with ART NOUVEAU, cannot be sampled below the melting temperature on the time scale available to molecular dynamics. They demonstrate that ART NOUVEAU is efficient with Stillinger-Weber in cSi, providing a clear picture of the energy landscape in agreement

with previously known results.[28–30] This being established, we can now turn to the central problem of this work, the formation of a SiO$_2$/Si interface.

IV. OXYGEN REACTION WITH A SILICON SUBSTRATE

In a previous study, we modeled the growth of silicon oxide on a silicon substrate using an algorithm that alternates between the inclusion of oxygen atoms according to empirical laws suggested by experimental results and *ab initio* calculations,[3,8,31] and atomic relaxations using molecular dynamics.[9] Although this method is convenient for generating a plausible SiO$_2$/Si interface, the hand-based insertion of oxygen, even following empirical rules, can introduce unknown biases in the system.

Here, we revisit our previous work using ART NOUVEAU, a procedure that allows the system to find its most stable state once oxygen atoms are placed on the surface of the Si substrate without external biases, focusing particularly on the early stages of the oxygen diffusion into the substrate.

To model the (Si,O) system, we use the semiempirical potential developed a few years ago by Watanabe *et al.*.[8] We refer the reader to the original paper for the details of this potential which extends on Stillinger-Weber. Our initial configuration is a 864-atom silicon bare substrate placed in simulation box of dimensions $23 \times 23 \times 32.6$ Å^3 with periodic boundary conditions applied in the x and y directions. On a nonreconstructed Si(001) surface perpendicular to the z direction, 36 oxygen atoms are deposited, positioned to saturate every available Si dangling bond [cf. Fig. 3(a)].

To focus on O diffusion, ART events are centered on the added oxygen atoms: an initial random displacement is imposed on a randomly selected oxygen atom and its
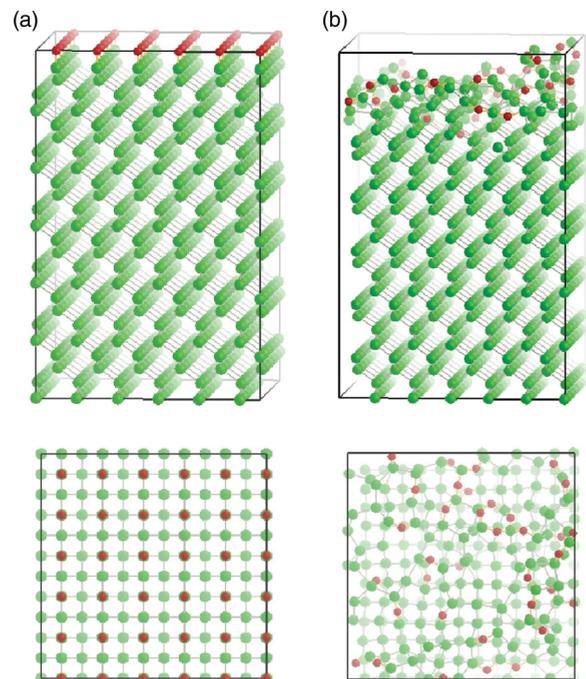

FIG. 3. (Color online) Profiles and top views of the system. (a) At the onset of the simulation, with the oxygen deposited on the surface. (b) At the end of one of the ART NOUVEAU simulations.
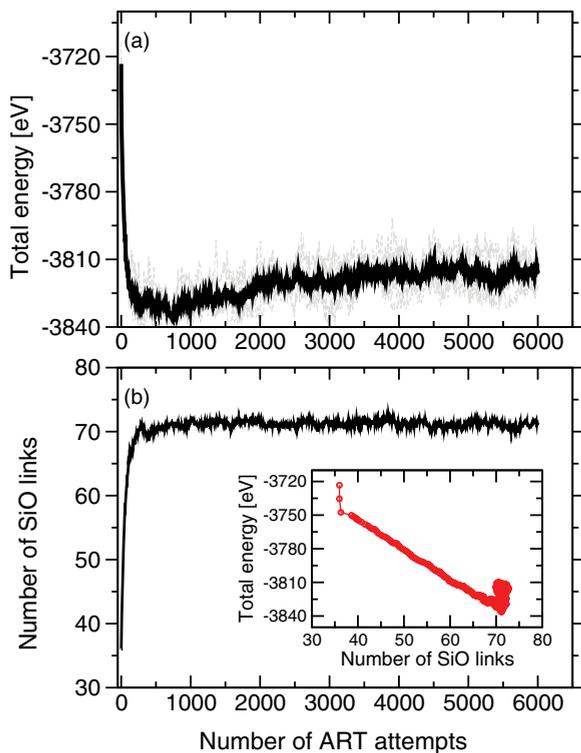
FIG. 4. (Color online) Evolution of (a) the total energy and (b) the number of SiO bonds as a function of event number averaged over the six independent trajectories. Inset: Total energy as a function of the number of SiO bonds.
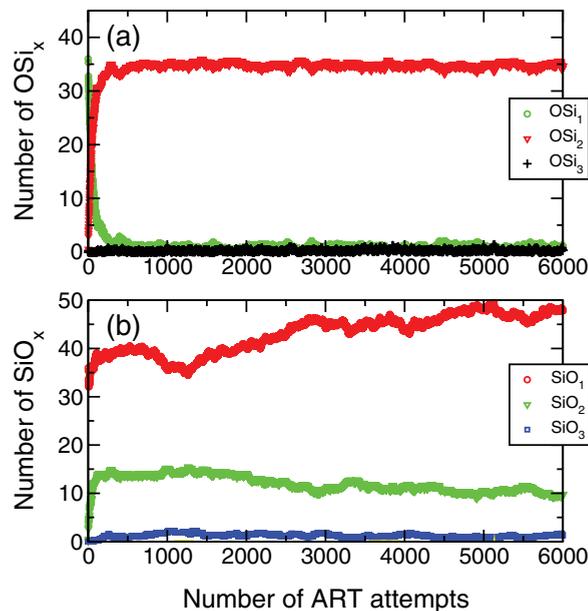

FIG. 5. (Color online) Evolution of the interspecies coordination numbers around (a) O and (b) Si atoms averaged over six independent simulations as a function of ART NOUVEAU events.

neighbors located within a surrounding sphere of 4 Å radius. The cutoff radius is selected to localize events essentially on the oxygen environment without preventing complex but physically relevant events. Tests realized with a larger cutoff radius showed that events involving Si atoms only dominate as self-defect diffusion requires lower energy barriers than for oxygen. To account for the higher asymmetry between the various states, we need to use a higher Metropolis temperature in the ART NOUVEAU scheme. As stated before, since ART does not include thermal entropic effects, this Metropolis variable does not correspond to a definite temperature.

Using these parameters, we launch six independent simulations, with a different sequence of pseudorandom numbers, and generate 6000 ART NOUVEAU events. During these simulations, events are accepted with a 29.6% probability, and the trajectories are long enough to reach stationary states. An example of a final configuration is showed in Fig. 3(b).

Starting from the initial configuration described above [Fig. 3(a)], oxygen atoms diffuse rapidly into the silicon substrate, disordering the top layers as they move into the bulk and forming an amorphouslike layer [Fig. 3(b)]. Figure 4(a) shows the evolution the total energy during the ART NOUVEAU simulations averaged over the six ART NOUVEAU trajectories. A rapid decrease in the total energy is observed in the first 600–700 events followed by a smooth increase as the system thermalizes. As shown in Fig. 4(b), the initial energy drop is correlated with a rapid increase in the number of SiO bonds as the oxygen atom reach a coordination of 2. The formation energy related to the formation of a SiO bond is ~3 eV per

formed bond [inset of the Fig. 4(b)]. Once the number of SiO bonds reaches an equilibrium value, oxygen migrations takes place through changes in the silicon substrate structure; these changes increase the total energy of the system without modifying the number of SiO bonds. As oxygen diffuse in, silicon atoms are displaced and interstitial Si atoms in the substrate as well as SiSi dimers on the surface are generated [Fig. 3(b)]. As we will see below, the energy minimum is observed as the oxygen atom moves into the top layers, forming SiO_2 configurations, the lowest energy structures. As the oxygen continue to diffuse in the bulk, the number of SiO_2 decreases, leading to a higher energy state corresponding to the effective temperature of the Metropolis accept/reject criterion.

Figures 5(a) and 5(b) present the evolution of the interspecies coordination numbers for O and Si atoms, respectively, during the burial of oxygen atoms within the silicon substrate. As shown in Fig. 5(a), oxygen atoms, initially onefold coordinated at the surface, become twofold coordinated to form SiOSi bonds as they move into the bulk and adopt a minimum-energy structure [Fig. 4(a)]. With the high Metropolis temperature used here, however, this structure is entropically unstable and oxygen atoms rapidly move further into the bulk, with a higher dominance of SiO_1 structures. During this process, we observe the presence of unstable threefold coordinated oxygen atoms that must be considered as intermediate species only, as should be expected. Regarding Si interspecies coordinations [Fig. 5(b)], starting with only onefold coordinated silicon at the initial condition, twofold and threefold coordinated silicon atoms forms during the procedure. Fourfold coordinated silicon atoms, i.e., SiO_4 entities, usually encountered in silicon oxide, can not be formed due to the small number of oxygen atoms involved in the systems.

The increase in the number of interspecies onefold coordinated silicon atoms is correlated with the formation of SiOSi bonds (twofold coordinated oxygen atoms) and SiSi dimers
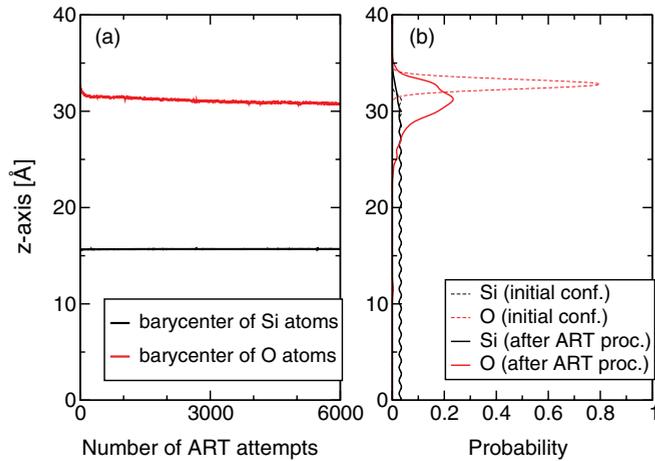
FIG. 6. (Color online) (a) Locations of the Si and O centers of mass along the z axis during the ART simulations and (b) positions of Si and O atoms along the z axis (broadened by a Gaussian with a standard deviation of 0.5 Å) before and after the ART run averaged over six independent simulations.

on the surface. The resulting oxide layer does not display any specific structural signature and should be considered as amorphouslike. As shown in Figure 6(a), which presents the evolution of the centers of mass location along the z axis for Si and O atoms during the ART simulations (averaged over the six trajectories), after a rapid displacement at the beginning of the run, the center of mass location of oxygen atoms shifts ~2 Å within the substrate as some silicon is pushed towards the surface. The distribution of Si and O atoms along the z axis, represented at the beginning and at the end of the procedure on Fig. 6(b) show that the oxygen spread over five silicon layers, with maxima in the first and second layers, in agreement with experimental data that show a relatively abrupt interface.

A. Energies' analysis

In the previous section, we showed that as oxygen diffuses into the bulk, the affected layers become amorphouslike. To understand the driving force behind this transformation, we look at the energy barriers associated with the events responsible for the local structural change.

Figure 7(a) presents the distribution of energy differences between the initial and the final minima ($\Delta E = E_f - E_i$) for all events. We find a continuous distribution that spreads from -6 eV to 6 eV and is characterized by a maximum at 0 eV and two satellites peaks at ~± 3.5 eV. The symmetry suggests that the distribution is dominated by the long stationary trajectories already discussed.

To correlate the variation in barrier energy with the structural evolution of the system, we compute the distribution of barrier heights calculated as a function of ΔE for energy windows of $\delta(\Delta E) = 0.5$ eV. Figure 7(b) presents the ΔE dependence of the projected distributions of energy barriers (in color scale). The dark blues region indicates well-defined barriers associated with the peaks observed in Fig. 7(a) suggesting that even though the system is disordered, its evolution is dominated by very specific diffusion mechanisms.
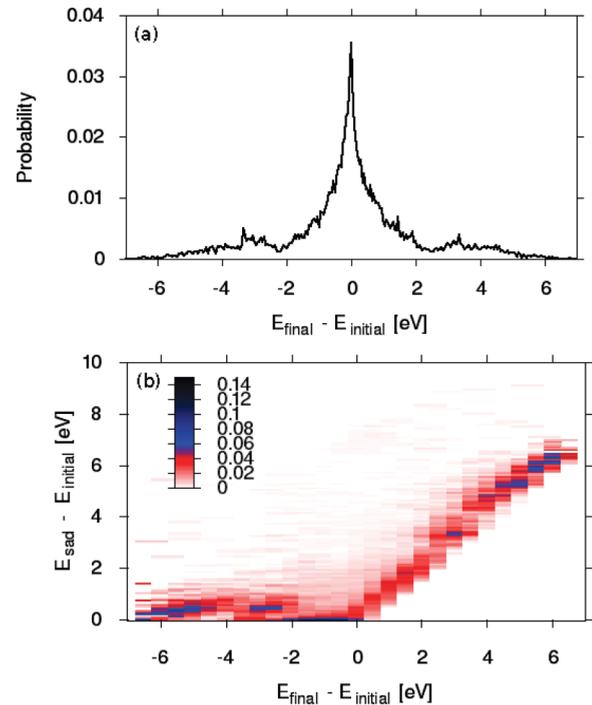

FIG. 7. (Color online) (a) Distribution of energy differences between the initial and the final minima obtained during the ART procedure for six independent runs. (b) Projected distributions of the barrier energies as a function of the asymmetry energy ($E_f - E_i$). The color coding indicates the probability as a function of barrier height.

We can identify these mechanisms by focusing on the distribution of the energy barriers computed for all events [Fig. 8(a)]. The wide distribution which can be decomposed in partial ones associated with a specific coordination change for the oxygen atoms. This decomposition allows us to identify the characteristic energy barrier of specific events: changes from OSi to OSi_2 [Fig. 8(b)], from OSi_2 to OSi [Fig. 8(c)], from OSi_2 to OSi_3 [Fig. 8(d)], from OSi_3 to OSi_2 [Fig. 8(e)], from OSi to OSi [Fig. 8(f)] and from OSi_2 to OSi_2 [Fig. 8(g)].

In terms of amplitude, the total distribution is dominated by jumps of twofold coordinated oxygen from one silicon atom to a neighboring one. This is not surprising as most oxygen atoms occupy such positions. These moves can be costly however, especially in the bulk where each atom is already fully coordinated, leading to a wide barrier distribution, with no real characteristic energy [Fig. 8(g)]. Moves that change the network are better defined, and a meaningful average energy barrier can be extracted from the barycenter of the distribution (Table II). We see that onefold or threefold oxygen move easily to twofold Si-O-Si conformations, with average barriers

TABLE II. Energy barriers of oxygen coordination changes.

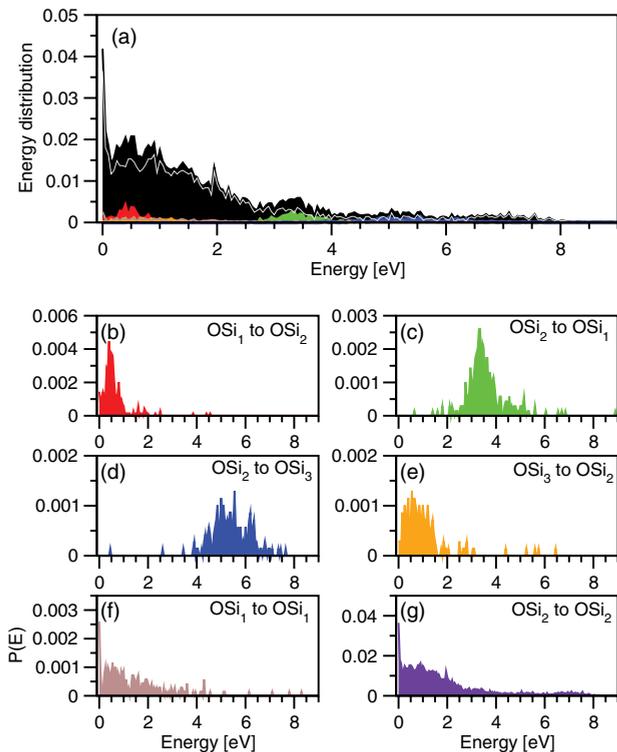| Events	Energy barrier (eV)
OSi_1 to OSi_2	0.62
OSi_2 to OSi_1	3.57
OSi_2 to OSi_3	5.38
OSi_3 to OSi_2	1.07

FIG. 8. (Color online) Distribution of energy barriers during the reaction of oxygen atoms with the silicon substrate as a function of the bonding environment. (a) All barriers (in black) as well as the individual ones shown separated in (b) to (g).

The method is then applied to model the reaction of an oxygen layer deposited on a silicon substrate. Contrary with our last investigation where empirical laws were used for inserting the oxygen atoms,[9,18] the present study using the ART NOUVEAU method allows the oxygen atoms to follow unbiased pathways to form SiO_2 oxide, providing new insights into the oxygen insertion.

While we start here with a single layer of oxygen at the surface, the local structural properties of the formed oxide obtained at the end of the simulations are consistent with our previous studies.[9,18] First, we observe a fast evolution of the system to optimize the oxygen coordination, through the formation of SiOSi bonds, and leading to the burial of this species. This leaves SiSi dimers on the surface which would disappear in a real system as new oxygen atoms are deposited.

This rapid burial leads to the formation of an abrupt SiO_2/Si interface as diffusion is slowed down significantly once the SiOSi are formed, a phenomenon that was observed using unsuitable empirical laws for inserting oxygen atoms,[18] but which is consistent with experimental observation:[7] oxygen atoms stay located on the top of the substrate and no specific long range structural signature is observed in the formed SiO_2 oxide.

This kinetics of formation can be understood by looking at the energy barriers between various coordination environments. An oxygen moving from a onefold to twofold coordinated state requires crossing a barrier of 0.6 eV while the opposite motion is associated with an energy barrier of 3.6 eV. A similar bias is observed for the very energetic threefold coordinated oxygens, which decay into a twofold state with a barrier of only 1.1 eV, while the reverse motion requires crossing a 5.4 eV barrier. This limits considerably the oxygen diffusion once a SiO_2 film is formed and deeper motion can only take place through silicon interstitial, which have been observed in the vicinity of the SiO_2/Si interface, or through more complex network rearrangements that preserve the oxygen coordination.

While these results clarify the very onset of the formation of the SiO_2/Si interface, further work is required to characterize better the mechanisms associated with the growth of this interface and processes, such as silicon interstitial injection in the substrate which is observed experimentally during silicon oxidization.[34] Having demonstrated the applicability of ART NOUVEAU to this problem, we can now consider methods, such as the kinetic activation-relaxation technique (kinetic ART), in order to provide a kinetic view of the process.[35,36]

between 0.7 and 1.1 eV while the opposite require crossing much higher barriers, between 4.6 and 5.4 eV.

This explains the facility with which the oxygen moves into the bulk in order to form a well-coordinated SiO_2 network: Once Si-O-Si bonds are created, the formation of onefold or threefold coordinated oxygen is strongly unfavorable. These energy barriers measured for the change of the oxygen coordination are consistent with experiment data[32] and recent *ab initio* calculations showing high values of activation energies for oxygen self-diffusion[33] and explain the observed narrow interface as moving from a Si-O-Si environment is very costly for the oxygen.

V. CONCLUSION

Using ART NOUVEAU[4–6] coupled with the Watanabe version of the Stillinger-Weber potential,[8] we simulate the insertion of oxygen deposited on the surface into a Si substrate. We first validate the ART NOUVEAU parameters by characterizing the diffusion mechanisms of single point defects in pure silicon, successfully recovering well-known results on vacancy diffusion and showing for interstitial diffusion that the migration between the most stable sites (EDI site) is mediated via an intermediary state (DI site).

[1] P. V. Smith and A. Wander, Surf. Sci. **219**, 77 (1989).

[2] J. Takizawa, S. Ohno, J. Koizumi, K. Shudo, and M. Tanaka, J. Phys.: Condens. Matter **18**, L209 (2006).

[3] D. Hojo, N. Tokuda, and K. Yamabe, Thin Solid Films **515**, 7892 (2007).

[4] G. T. Barkema and N. Mousseau, Phys. Rev. Lett. **77**, 4358 (1996).

[5] R. Malek and N. Mousseau, Phys. Rev. E **62**, 7723 (2000).

[6] E. Machado-Charry, L. K. Béland, D. Caliste, L. Genevese, T. Deutsch, N. Mousseau, and P. Pochet, J. Chem. Phys. **135**, 034102 (2011).

[7] Y. Zhao, H. Matsumoto, T. Sato, S. Koyama, M. Takenaka, and S. Takagi, IEEE Trans. Electron Devices **57**, 2057 (2010).

[8] T. Watanabe, H. Fujiwara, H. Noguchi, T. Hoshino, and I. Ohdomari, Jpn. J. Appl. Phys. **38**, L366 (1999).

[9] P. Ganster, G. Tréglia, and A. Saúl, Phys. Rev. B **81**, 045315 (2010).

[10] A. Hemeryck, A. Esteve, N. Richard, M. Djafari Rouhani and Y. J. Chabal, Phys. Rev. B **79**, 035317 (2009).

[11] N. Mousseau and G. T. Barkema, Phys. Rev. E **57**, 2419 (1998).

[12] N. Mousseau, G. T. Barkema, and S. W. de Leeuw, J. Chem. Phys. **112**, 960 (2000).

[13] H. Kallel, N. Mousseau, and F. Schiettekatte, Phys. Rev. Lett. **105**, 045503 (2010).

[14] M.-C. Marinica, F. Willaime, and N. Mousseau, Phys. Rev. B **83**, 094119 (2011).

[15] E. Cances, F. Legoll, M.-C. Marinica, K. Minoukadeh, and F. Willaime, J. Chem. Phys. **130**, 114711 (2009).

[16] F. H. Stillinger and T. A. Weber, Phys. Rev. B **31**, 5262 (1985).

[17] T. Watanabe, K. Tatsumura, and I. Ohdomari, Appl. Surf. Sci. **237**, 125 (2004).

[18] P. Ganster, G. Tréglia, A. Saúl, F. Lançon and P. Pochet, Thin Solid Films **518**, 2422 (2010).

[19] K. Tatsumura, T. Shimura, E. Mishima, K. Kawamura, D. Yamasaki, H. Yamamoto, T. Watanabe, M. Umeno, and I. Ohdomari, Phys. Rev. B **72**, 045205 (2005).

[20] S. R. Billeter, A. Curioni, D. Fischer, and W. Andreoni, Phys. Rev. B **73**, 155329 (2006).

[21] D. J. Cole and M. Payne, J. Chem. Phys. **127**, 204704 (2007).

[22] J. Yu, S. B. Sinnott, and S. R. Phillpot, Phys. Rev. **75**, 085311 (2007).

[23] A. C. T. van Duin, A. Strachan, S. Stewman, Q. Zhang, X. Xu, and W. A. Goddard, J. Phys. Chem. A **107**, 3803 (2003).

[24] P. Philipp, L. Briquet, T. Wirtz, and J. Kieffer, Nucl. Instrum. Methods B. **269**, 1555 (2011).

[25] P. J. Ungar, T. Halicioglu, and W. A. Tiller, Phys. Rev. B **50**, 7344 (1994).

[26] G. H. Gilmer, T. Diaz de la Rubia, D. M. Stock, and M. Jaraíz, Nucl. Instr. and Meth. B **102**, 247 (1995).

[27] P. Ganster, G. Tréglia, and A. Saúl, Phys. Rev. B **79**, 115205 (2009).

[28] H. R. Schober, Phys. Rev. B **39**, 13013 (1989).

[29] M. Nastar, V. V. Bulatov, and S. Yip, Phys. Rev. B **53**, 13521 (1996).

[30] M. Posselt, F. Gao, and H. Bracht, Phys. Rev. B **78**, 035208 (2008).

[31] F. Fuchs, W. G. Schmidt, and F. Bechstedt, J. Phys. Chem. B **109**, 17649 (2005).

[32] J. C. Mikkelsen, Appl. Phys. Lett. **45**, 1187 (1984).

[33] L. Martin-Samos, G. Roma, P. Rinke, and Y. Limoge, Phys. Rev. Lett. **104**, 075502 (2010).

[34] B. Leroy, Philos. Mag. **55**, 159 (1987).

[35] F. El-Mellouhi, N. Mousseau, and L. J. Lewis, Phys. Rev. B **78**, 153202 (2008).

[36] L. K. Béland, P. Brommer, F. El-Mellouhi, J.-F. Joly, and N. Mousseau, Phys. Rev. E **84**, 046704 (2011).